

Measurements of ballistic transport at nonuniform magnetic fields in cross junctions of a curved two-dimensional electron gas

K.-J. Friedland,* R. Hey, H. Kostial, A. Riedel, and K. H. Ploog

Paul-Drude-Institut für Festkörperelektronik, Hausvogteiplatz 5-7, 10117 Berlin, Germany

(Received 17 July 2006; published 31 January 2007)

We investigate ballistic transport in a high-mobility, two-dimensional electron gas, which is rolled up as a tube. The distinctiveness of our structure is that the electron's mean free path is as large as the radius of the tube. As a result free electron trajectories bend in space by about 60° while being confined in the curved quantum well. We observe negative bend resistances at zero magnetic field in cross junctions. In addition, the bend resistance becomes strongly asymmetric with respect to the orientation of the magnetic field due to varying magnetic field along the junction. The resistance asymmetry at low fields arises from trochoidlike trajectories, which carry electrons in the opposite direction as compared to the direction of conventional guided trajectories. At high magnetic fields, the interaction between closely separated channels of opposite velocity determines the bend resistance at the transition between integer filling factors.

DOI: [10.1103/PhysRevB.75.045347](https://doi.org/10.1103/PhysRevB.75.045347)

PACS number(s): 73.23.Ad, 73.43.Fj, 73.90.+f

I. INTRODUCTION

Free-standing semiconductor heterojunctions are of considerable interest for fundamental research areas, such as current-induced spin polarization¹ and optics in microtube ring resonators.² The self-rolling of thin pseudomorphically strained semiconductor bilayer systems based on epitaxial heterojunctions grown by molecular-beam epitaxy (MBE) as proposed by Prinz and co-workers³ allows one to realize motion of electrons on curved surfaces. For such an extreme experiment there are two complementary points of interest: one is how the electron motions are affected by the local curvature of the surface. The other is how the global topology affects quantum-mechanical wave functions, as emphasized by Aoki *et al.*⁴ For the first problem, the electron motion in an effectively nonuniform normal-to-surface component of the magnetic field is the most dominant modification. A new class of electron trajectories, such as snake-like trajectories, were proposed to exist in ballistic mesoscopic structures with nonuniform magnetic fields.⁵

To study the relevant ballistic motion in a curved two-dimensional electron gas (2DEG), the low-temperature mean free path of the electrons l_S should be comparable not only with the typical structure size, but also with the curvature radius R . To realize large values of l_S , high-mobility 2DEG's based on (Al,Ga)As heterojunctions are typically used. However, a significant drawback for free-standing (Al,Ga)As heterojunctions is the Fermi-level pinning in the gap due to the inherent formation of the new surface which results in a partial depletion of the 2DEG accompanied by enhanced fluctuations of the potential and, therefore, by a reduced mobility of the 2DEG.

To overcome this deterioration of the mobility, we use a particular heterojunction grown by MBE, where the high-mobility 2DEG is located in a 13-nm-wide single quantum well (SQW) with barriers consisting of short-period AlAs/GaAs superlattices (SPSL's).⁶ The superlattice period is chosen sufficiently short in order to ensure that the X -like conduction-band states are lowest in energy in the AlAs compound of the SPSL's. The heavy mass of the carriers

provides a high screening capability. In addition, their Bohr radius and their nominal distance from the doping layer are smaller or nearly equal to the average distance between the Si atoms in the δ -like doping plane. Therefore, the X electrons effectively smooth the fluctuations of the scattering potential. In addition, at low temperatures, the X electrons do not contribute to the conductivity. As a result, the mobility of the electrons in the GaAs SQW with X electrons in the SPSL can be considerably increased. The current concept for rolled up films is that these X electrons also screen the high-mobility 2DEG from depleting states at the new surface.

II. EXPERIMENT

The layer stack, including the high-mobility 2DEG with an overall thickness of 192 nm, was grown on top of a 20-nm-thick $\text{In}_{0.15}\text{Ga}_{0.85}\text{As}$ stressor layer, an essential component of strained multilayered film (SMLF). An additional 50-nm-thick AlAs sacrificial layer is introduced below the SMLF in order to enable the separation of the SMLF from the substrate.

For the fabrication of curved 2DEG's, we first shaped conventional Hall bar structures in the flat heterojunction along the [010] direction. The two 20- μm -wide Hall bar arms and three opposite 4- μm -wide lead pairs—separated by 10 μm —are connected to large Ohmic contact pads outside of the rolling area, similarly to the recently developed technology for fabrication of laterally structured and rolled up 2DEG's with Ohmic contacts.^{7,8} In a next step, the SMLF including the Hall bar was released by selective etching of the sacrificial AlAs layer with a 5% HF acid/water solution at 4 °C starting from an [010] edge. By relaxing the strain, the SMLF rolls up along the [100] direction, forming a complete tube with a radius of about 20 μm . We report on structures which have a carrier density of $(6.8\text{--}7.2) \times 10^{15} \text{ m}^{-2}$ and a mobility up to 90 $\text{m}^2(\text{V s})^{-1}$ along the [010] crystal direction before and after rolling-up. Note that the magnetoresistance is already anisotropic in the unrolled high-mobility 2DEG due to anisotropic interface

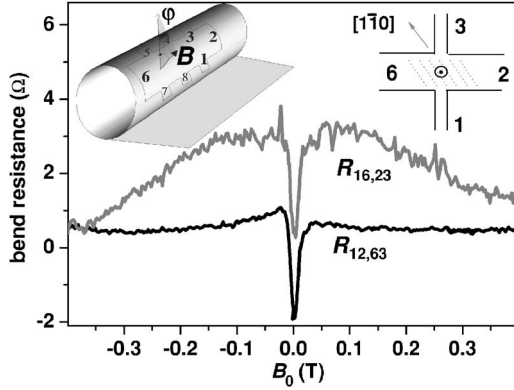


FIG. 1. Bend resistances in a cross junction with a magnetic field \mathbf{B} normal to the surface at the center of the junction—i.e., $\varphi=0^\circ$ at $T=0.3$ K. The insets demonstrate schematically the geometry of our experiments. The right inset shows the direction of the interface corrugations along $[1\bar{1}0]$.

corrugations⁹—the mobility along $[1\bar{1}0]$ is nearly 2 times larger than the one along $[010]$.

III. RESULTS AND DISCUSSION

As a result, we obtain curved high-mobility 2DEG structures, which are just as wide as their curvature radius. In addition, the electron's mean free path is as large as its curvature radius. Consequently, for an electron motion along the curvature free electron trajectories bend in space by about 60° while being confined in the curved quantum well.

The high mobility in our structures allows for the observation of a new class of trajectories in the ballistic motion of electrons in curved 2DEG's. To demonstrate the ballistic carrier motion, we investigate the magnetoresistance in cross junctions that are formed by two opposite narrow leads in the Hall bar. The Hall bar is aligned along the tube axis. In this way, this experiment resembles the four-terminal nonlocal ballistic resistance measurement at two opposite quantum point contacts (QPC's).¹⁰ Here, in addition, the magnetic field component perpendicular to the surface changes along the circumference of the curved 2DEG—i.e., along the direction of the narrow leads. We measure the resistance $R_{ij,kl}$ which indicates the current flow along the leads i and j , while the voltage is measured between the leads k and l . The experimental layout is schematically demonstrated by the insets in Figs. 1 and 2.

A. Ballistic transport in a curved 2DEG, symmetric case

First, we consider the configuration, where the magnetic field B is perpendicular to the surface at the center of the Hall bar arc. With a curvature radius of about $20\ \mu\text{m}$, the $20\text{-}\mu\text{m}$ -wide Hall bar spans over $\Delta\varphi=57^\circ$. Correspondingly, the perpendicular magnetic field components $B_\perp=B_0\cos(\varphi)$ at the narrow lead positions are only by 12% lower than B_0 . Figure 1 illustrates the results of the ballistic four-terminal magnetotransport measurement, which are qualitatively similar in the flat, unrolled cross junctions. The curves are sym-

metric with respect to the orientation of the magnetic field, indicating the absence of dominant spatial defects in the studied cross junctions. At zero magnetic field, the bend resistance $R_{12,63}$ is negative, indicating the preferential transmission of electrons into the opposite leads instead of being scattered into the side arms of the junction.¹¹ We estimate the negative bend resistance R_{NBR} by calculating the number of channels $N=k_F W/\pi$ in the leads, where k_F is the Fermi wave number and W the width of the leads, assuming a collimation factor $f\approx 1$ (Ref. 10):

$$R_{NBR} = R_{12,63}(B_0=0) = \frac{h}{2e^2} \left(f^2 - \frac{1}{2} \right) \frac{\pi}{2k_F W} \approx 12\Omega. \quad (1)$$

This value may become larger when we take into account a lower number of injected channels at the QPC due to carrier depletion from the boundaries. However, the density is rather high in the present SQW so that we do not expect a significant reduction of the number of channels in the QPC. For different samples and transversal Hall-terminal pairs, we measure negative bend resistances of about $2\text{--}6\ \Omega$, indicating that a certain part of the trajectories is still reflected into the side arms of the cross junction. The bend resistance in the other direction, $R_{16,23}$, is usually not negative at $B_0=0$, indicating a much stronger side-arm transmission of carriers in this configuration. Nevertheless, a similarly strong resistance dip around $B_0=0$ is also observed in this configuration. In order to understand this difference, we stress the resistance anisotropy in the present SQW due to anisotropic interface corrugations, which we indicate in the right inset of the Fig. 1 by dotted lines.

To model the bend and Hall resistances R_B and R_H we use in accordance with Ref. 12 the Landauer-Büttiker formalism, in which the transmission coefficients T_{ij} from lead i to lead j are used to calculate the four-terminal resistances. In particular, for junctions with four-fold symmetry, one obtains¹²

$$R_B^{LB} = \frac{h}{2e^2} \frac{T_L T_R - T_F^2}{D}, \quad (2)$$

where T_L , T_R , and T_F denote the left- and right-turning and forward transmission coefficients, respectively, $D=(T_R+T_L)[T_R^2+T_L^2+2T_F(T_R+T_L+T_F)]$. In order to consider the conductance anisotropy, we assume that the transmission coefficients differ for different directions. We indicate by T_{ij} and \tilde{T}_{ij} the coefficients that describe the transmission mainly along $[1\bar{1}0]$ and $[110]$, which are the high- and low-mobility directions, respectively. In addition, we mark by \tilde{T}_F and T_F the forward transmission coefficients into the narrow and wide leads, respectively. As a result we obtain for the bend resistances

$$R_{12,63}^{LB} = \frac{h}{2e^2} \frac{T_L T_R - T_F \tilde{T}_F}{D}, \quad R_{16,23}^{LB} = \frac{h}{2e^2} \frac{\tilde{T}_L \tilde{T}_R - \tilde{T}_F T_F}{D}, \quad (3)$$

with $D=(T_R+\tilde{T}_L)[T_R\tilde{T}_R+T_L\tilde{T}_L+\tilde{T}_F(T_R+\tilde{T}_L+T_F)+T_F(\tilde{T}_R+T_L+\tilde{T}_F)]$. The zero-field negative bend resistance $R_{12,63}$ indicates that $T_L T_R < T_F \tilde{T}_F$ at $B_0=0$. By applying a low magnetic

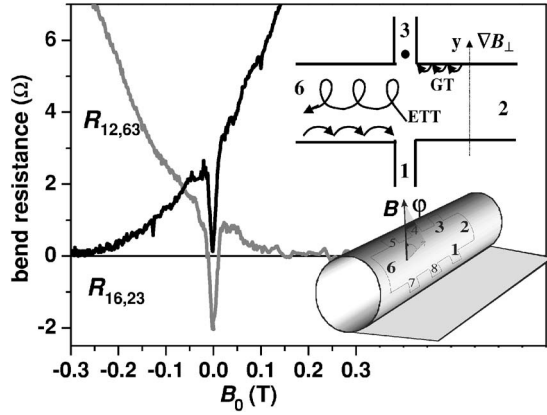


FIG. 2. Bend resistances in a cross junction with a magnetic field B perpendicular to the surface at lead 3—i.e., $\varphi=29^\circ$ —at $T=0.3$ K. The inset schematically shows extended trochoidlike (ETT) and guided (GT) trajectories.

field, \tilde{T}_F decreases due to deflection of the electron beam from the opposite narrow QPC and vanishes eventually at a magnetic field, for which the cyclotron radius $L_C = 2\pi k_F / (eB)$ is comparable to the width of the Hall bar. At the same time, $T_L T_R$ goes to zero because one of the T_{ij} decreases at the expense of the other. The finite positive value of $R_{16,23}$ at intermediate magnetic fields forming the compensating background for R_B at $B_0=0$ indicates additional scattering for transmission in the $[110]$ direction. In this case, electrons are more equally distributed into the left- and right-turning states so that $\tilde{T}_L \tilde{T}_R$ becomes finite and disappears only at magnetic fields of about $B_0 \cong 0.3$ T, for which L_C is comparable to the correlation length of the potential fluctuations.⁹

B. Ballistic transport in a curved 2DEG, nonsymmetric case

We observe a dramatically different behavior when the magnetic field is tilted away from the surface normal at the center of the Hall bar arc by an angle φ . Figure 2 shows $R_{12,63}$ and $R_{16,23}$ as a function of the magnetic field for $\varphi=29^\circ$. In this case, the magnetic-field gradient along the circumference becomes much larger, than the one for the $\varphi=0^\circ$ case. The perpendicular magnetic field component is more than 2 times larger on the high-magnetic-field side of the Hall bar, at lead 3, as compared to the low-magnetic-field side, at lead 1. As a result, the magnetoresistance becomes extremely asymmetric with respect to the orientation of the magnetic field, which is not observed in unrolled flat samples. $R_{12,63}$ is zero for high positive magnetic fields, while the resistance turns to negative values at $B_0=0$. In contrast, by reversing the direction of the magnetic field, a positive resistance $R_{12,63}$ appears, which increases monotonically with $|B_0|$. In accordance, $R_{16,23}$ becomes nearly the mirror image of $R_{12,63}$ with respect to the field direction. However, $R_{16,23}$ is not negative at $B_0=0$. Nevertheless, a dip in $R_{16,23}$ also exists, which is comparable to the low-field dip of $R_{12,63}$.

An asymmetric resistance—with respect to the field direction—in curved 2DEG's was already observed in the

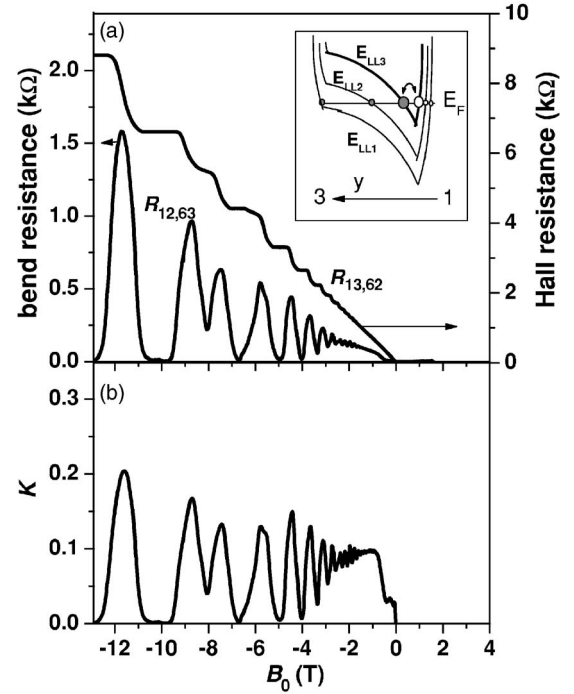


FIG. 3. (a) Bend and Hall resistances in a cross junction with a magnetic field B perpendicular to the surface at lead 3—i.e., $\varphi=29^\circ$ —at $T=0.3$ K. The inset schematically shows the Landau-level energies along the field gradient. One-dimensional edge states and 1DLC's are indicated by circles and dots, respectively. (b) The fraction K of oppositely directed trajectories as represented by the ratio of the bend and Hall resistances $R_{12,63}/R_{13,62}$.

longitudinal resistance in the quantum Hall effect and was interpreted by bending of one-dimensional Landau channels (1DLC's) from the edge into the bulk due to magnetic barriers.^{13,14} The effective potential in nonuniform magnetic fields results in a one-dimensional charge flow along the direction perpendicular to the field gradient,⁵ which in our case corresponds along the wide Hall bar arms between leads 2 and 6. We observe the asymmetric resistance already at very low fields in the ballistic transport regime, where edge states are not formed yet. Instead, part of the ballistic trajectories of the electron motion are modified by an instantaneous varying cyclotron radius L_C , resulting in open trajectories. In particular, as indicated in Fig. 2, extended trochoidlike trajectories (ETT's) form, which drift perpendicularly to the field gradient.⁵ The drift direction is the same as for the guided trajectories (GT's) on the high-magnetic-field side and consequently opposite to the guided trajectories on the low-magnetic-field side of the Hall bar.

We suppose that part of the electrons, which are injected from lead 1 on the low-magnetic-field side, move as ETT. In dependence on the magnetic field direction, they transfer into the left or right arm of the Hall bar with probability T_L^{ETT} or T_R^{ETT} . The directions of corresponding GT—with probability T_R^{GT} or T_L^{GT} —are opposite. Consequently, in the framework of transmission rates, this results in nonzero values of $T_R^{GT} T_L^{ETT}$ and $T_L^{GT} T_R^{ETT}$ for the corresponding magnetic field directions, for which T_R^{GT} and T_L^{GT} are nonzero. For example, at sufficiently large negative magnetic fields, when $\tilde{T}_F \approx 0$ but

$T_R^{GT} > 0$, we obtain a nonzero bend resistance

$$R_{12,63}^{LB} = \frac{h}{2e^2} \frac{T_R^{GT} T_L^{ETT}}{\tilde{D}} > 0, \quad (4)$$

with $\tilde{D} = (T_R^{GT} + T_L^{ETT})[T_R^{GT} \tilde{T}_R^{GT} + T_L^{ETT} T_L^{ETT} + T_F(\tilde{T}_R^{GT} + T_L^{ETT})]$. In contrast, $R_{12,63}^{LB} = 0$ at $B_0 > 0$, when $T_R^{GT} = 0$ and vice versa. For the Hall resistance, we calculate

$$R_{13,26}^{LB} = \frac{h}{2e^2} \frac{T_R^{GT}(T_R^{GT} + T_L^{ETT}) - \tilde{T}_L^{GT}(\tilde{T}_L^{GT} + T_R^{ETT})}{\tilde{D}}. \quad (5)$$

C. Quantum Hall effect

At high magnetic fields, the quantum Hall effect becomes evident as quantum Hall plateaus in R_H and zeros in R_B around the plateau positions as shown in Fig. 3(a). In fact, the analysis of the four-terminal resistances in the quantum Hall effect by the Landauer-Büttiker approach for the present geometry results in zero R_B just at integer filling factors, despite the existence of 1DLC's within the Hall bar. These 1DLC's arise at the positions where the Fermi energy crosses the Landau-level energies E_{LL} —as demonstrated in the inset of Fig. 3(a)—and extend from lead 2 to lead 6, leaving aside leads 1 and 3. By increasing the magnetic field, the 1DLC's move towards the low-field side of the Hall bar, here lead 1. Eventually, the 1DLC's come close to the innermost edge channel before disappearing. Consequently, this narrowing of the two one-dimensional channels with opposite electron velocities enhances the interaction and determines the transition from one filling factor to the next. In particular, this interaction leads to a probability for transfer of electrons to

the left, while injected into the right-turning edge state and vice versa. The strong increase of R_B with increasing magnetic field is due to a decreasing number of involved channels. This is actually the same scheme as for nonzero and antisymmetric bend resistances as presented by Eq. (4). For cross junctions with a magnetic field gradient, these open channels at low magnetic fields are therefore regarded as a precursor for the 1DLC's in the bulk at high magnetic fields. We estimate the part K of oppositely directed states by calculating the fraction $K = R_{12,63}/R_{13,62} \approx T_L^{ETT}/(T_R^{GT} + T_L^{ETT})$ in accordance with Eqs. (4) and (5); see Fig. 3(b). For low magnetic fields, K represents the fraction of trochoidlike ballistic trajectories, while at high magnetic fields K counts the oppositely transferred carriers in the transition region between two filling factors.

IV. CONCLUSION

In conclusion, we have demonstrated ballistic transport in curved 2DEG's when the electron's mean free path is as large as the radius of the tube. This opens the way to investigate the motion of electrons on nontrivial curved surfaces and the global topology affects on quantum-mechanical wave functions. Here, we demonstrated the existence of open ballistic trajectories as precursor for one-dimensional channels in the bulk due to crossing of the Landau-level energies with the Fermi energy.

ACKNOWLEDGMENTS

The authors gratefully acknowledge stimulating discussions with Y. Takagaki, H. T. Grahn, and V. Prinz. We thank E. Wiebicke and M. Hörnicke for technical assistance.

*Corresponding author. Electronic address: kjf@pdi-berlin.de

- ¹Y. K. Kato, R. C. Myers, A. C. Gossard, and D. D. Awschalom, Phys. Rev. Lett. **93**, 176601 (2004).
- ²T. Kipp, H. Welsch, Ch. Strelow, Ch. Heyn, and D. Heitmann, Phys. Rev. Lett. **96**, 077403 (2006).
- ³V. Ya Prinz, V. A. Seleznev, A. K. Gutakovskiy, A. V. Chehovskiy, V. V. Preobrazhenskii, M. A. Putyato, and T. A. Gavrilova, Physica E (Amsterdam) **6**, 828 (2000).
- ⁴H. Aoki, M. Koshino, D. Takeda, H. Morise, and K. Kuroki, Phys. Rev. B **65**, 035102 (2001).
- ⁵J. E. Müller, Phys. Rev. Lett. **68**, 385 (1992).
- ⁶K.-J. Friedland, R. Hey, H. Kostial, R. Klann, and K. Ploog, Phys. Rev. Lett. **77**, 4616 (1996).
- ⁷A. B. Vorob'ev, V. Ya. Prinz, Yu. S. Yukecheva, and A. I. Toropov, Physica E (Amsterdam) **23**, 171 (2004).
- ⁸S. Mendach, O. Schumacher, Ch. Heyn, S. Schnell, H. Welsch,

and W. Hansen, Physica E (Amsterdam) **23**, 274 (2004).

- ⁹K.-J. Friedland, R. Hey, O. Bierwagen, H. Kostial, Y. Hirayama, and K. H. Ploog, Physica E (Amsterdam) **13**, 642 (2002).
- ¹⁰A. S. D. Heindrichs, H. Buhmann, S. F. Godijn, and L. W. Molenkamp, Phys. Rev. B **57**, 3961 (1998).
- ¹¹Y. Takagaki, G. Gamo, S. Namba, S. Ishida, S. Takaoko, K. Murase, K. Ishibashi, and Y. Aoyagi, Solid State Commun. **68**, 1051 (1988).
- ¹²H. U Baranger, D. P. DiVincenzo, R. A. Jalabert, and A. D. Stone, Phys. Rev. B **44**, 10637 (1991).
- ¹³A. B. Vorob'ev, K.-J. Friedland, H. Kostial, R. Hey, Yu. S. Yukecheva, U. Jahn, E. Wiebicke, and V. Ya. Prinz (unpublished).
- ¹⁴S. Mendach, Ph.D. dissertation, Fachbereich Physik, Universität Hamburg, 2005.